Mathematical Theory and Modeling
ISSN 2224-5804 (Paper) ISSN 2225-0522 (Online)
Vol.8, No.7, 2018

Effect of Viscous Dissipation on Natural Convection Flow in a Vertical Parallel-Plate Microchannel with Suction and Injection

Abiodun O. AJIBADE[1], Donald O. OTOR[2*], OLOM, P. Ogbo[2] & ONAH, O. Francis[2]
1. Department of Mathematics, Ahmadu Bello University, Zaria, Nigeria
2. Department of Mathematics, College of Education, Oju, Benue State, PMB 2035, Otukpo.
* donaldomenka@gmail.com

Abstract
This paper investigates the effects of viscous dissipation on the hydrodynamic and thermal behaviour of a fully developed natural convection flow in a vertical parallel–plate microchannel with suction and injection by the Homotopy perturbation method. The velocity slip and temperature jump conditions at the walls are taken into account. The influence of viscous dissipation (Ec) on the microchannel hydrodynamic and thermal behaviour was discussed with the aid of graphs. The study reveals that the presence ($Ec > 0$) and variation of viscous dissipation parameter in natural convention flow significantly affects the microfluidic system of infinite length and should not be neglected.

Keywords: Natural convection, viscous dissipation, suction and injection.

1. Introduction

Heat transfer by natural convection frequently occurs in many physical problems and engineering applications such as geothermal systems, heat exchangers, chemical catalytic reactors, fiber and granular insulation, packed beds, petroleum reservoirs, and nuclear waste repositories (Kargar and Arkbarzade, 2012) and so on. In particular, devices having their dimension of microns have been used in many fields such as biomedicine, diagnostics, chemistry, electronics, automotive industry, space industry, and fuel cells. With the increase in integrated circuit density and power dissipation of electronic devices, it is becoming more necessary to employ effective cooling devices, and cooling methods to maintain the operating temperature of electronic components at a safe level. Especially when device dimension gets smaller, overheating of microelectronic components may be a serious issue (Kakac, *et al.*, 2010). This pressing requirement of cooling of electronic devices has initiated extensive research in microchannel heat transfer.

High velocity gradients exist in channels with small hydraulic diameters, especially in flows through conventionally-sized microchannels of infinite lengths; hence, viscous dissipation becomes a non-negligible phenomenon in such fluid flow (Kakac *et al.*, 2010). Chen and Weng (2005) theoretically investigated natural convection in a vertical microchannel, taking into consideration the velocity slip and temperature jump conditions at the walls. Haddad *et al.* (2005) studied the developing free convection gas flow in a vertical open ended microchannel with porous media. Shojaefard *et al.* (2005) investigated flow control on a subsonic airfoil by suction/injection and concluded that suction significantly increases lift coefficient while injection decreases the surface skin friction, which transitively resulted in a considerable reduction in energy consumed during flights of subsonic aircrafts. Jha and Ajibade (2010) studied the effects of suction/injection on free convective motion of a viscous incompressible fluid between two periodically heated infinite vertical parallel-plates and found that temperature increases near the plate with injection while velocity is enhanced near the plate with suction. Jha *et al.* (2013) studied the effects of suction and injection on natural convection flow in a vertical parallel-plate microchannel. In their study, the effects of fluid-wall interaction, rarefaction, and ambient wall temperature difference were included. The study finds out that as suction and injection on the channel surfaces increases, the volume flow rate increases and the rate of heat transfer decreases.

On the other hand, Takhar and Beg (1997) have modelled viscous dissipation in the porous medium past a vertical porous plate, while, Murthy and Singh (1997) modelled the flow of an incompressible fluid in a saturated porous medium, with the effect of viscous dissipation included. The effect of viscous dissipation on the development of boundary layer flow from a cold vertical surface embedded in a Darcian porous medium was investigated by Rees *et al* (2003). Nield (2007) made a critical review of recent studies on the modelling of viscous dissipation in a saturated porous medium, with application to either forced convection or natural convection. Uddin *et al.* (2013) analyzed the influence of viscous dissipation on free convective boundary layer flow of a non-Newtonian power law nanofluid over an isothermal vertical flat plate embedded in a porous

[1] E-mail: olubadey2k@yahoo.com
[2] Correspondences: donaldomenka@yahoo.com

medium. The effects of suction, viscous dissipation, thermal radiation and thermal diffusion on a boundary flow of nanofluids over a moving flat plate have been discussed by Motsumi and Makinde (2012). Vahid *et al.* (2011) studied the slip flow heat transfer in circular microchannel with viscous dissipation, while Tunc and Bayazitoglu (2002) studied the effects of viscous dissipation for rarefied gas flow in slip-flow regime in circular and rectangular microchannels. They concluded that viscous dissipation plays an important role in the heat transfer through microdevices and also for gas flow.

The present study seeks to extend the work of Jha *et al.* (2013) to include the effect of viscous dissipation in the flow configuration. This extension is predicated on the fact that, as fluid particles flow in mass with continuous interactions of adjacent layers, the work done against viscous forces is irreversibly converted into internal energy in a viscous fluid per unit volume, and may significantly affect the characteristic behaviour of micro-fluidic and thermal systems. By considering the viscous dissipation term in the present study, the governing equations of velocity and temperature become nonlinear and coupled such that solutions by exact methods are not feasible. However, solutions of such equations are obtainable by some numerical or approximate analytical approaches, amongst which is the Homotopy perturbation method (HPM) adopted in this study.

2. Mathematical Analysis

The present problem considers a fully developed steady natural convection flow of a fluid in a microchannel formed by two infinite vertical parallel-plates of distance b apart. A coordinate system is chosen such that the x-axis is parallel to the gravitational acceleration g but in opposite direction, while the y-axis is orthogonal to the channel walls. The plates are heated asymmetrically with one plate maintained at a temperature T_1 and the other plate at a temperature T_2 where $T_1 > T_2$. Due to this temperature difference between the plates, natural convection flow occurs in the channel. In addition, fluid is being injected into the flow region through the plate with temperature T_2 and in order to conserve the mass of fluid in the channel, fluid is being sucked out at the same velocity V_0 through the plate with temperature T_1. The plates are defined by $y = 0$ and $y = 1$ respectively. The schematic representation of the system and of the coordinate axes is shown in figure1.

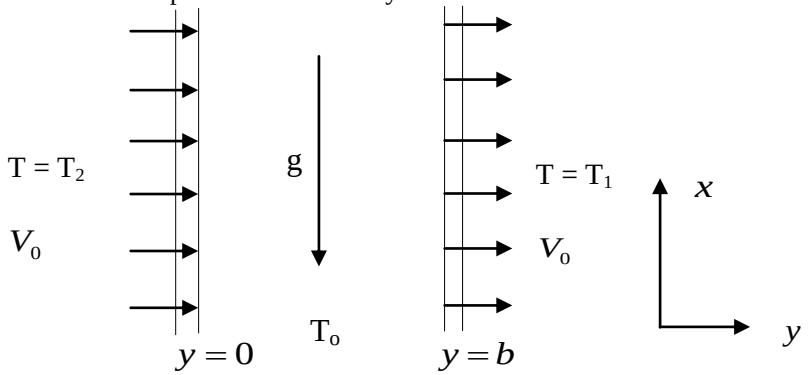

Figure 1: flow configuration and coordinate system.

2.1 Governing equations

The governing equations in dimensionless form for the transport processes in the presence of velocity slip and temperature jump conditions are given by:

$$\frac{d^2U}{dY^2} - s\frac{dU}{dY} + \theta = 0 \tag{1}$$

$$\frac{d^2\theta}{dY^2} - s\,\mathrm{Pr}\frac{d\theta}{dY} + Ec.\mathrm{Pr}\left(\frac{dU}{dY}\right)^2 = 0 \tag{2}$$

following the dimensionless quantities:

$$Y = \frac{y}{b},\ \theta = \frac{T - T_o}{T_1 - T_0},\ s = \frac{V_0 b}{\nu},\ U = \frac{u}{U_0},\ P_r = \frac{\nu}{\alpha},\ Ec = \frac{U_0^{\,2}}{c_p(T_1 - T_0)},$$

where

$$U_0 = \frac{\rho g \beta (T_1 - T_0) b^2}{\mu} \tag{3}$$

The dimensionless boundary conditions which describe velocity slip and temperature jump conditions at the fluid-wall interface are given by:

$$U(0) = \beta_v kn \frac{dU(0)}{dY}, \qquad U(1) = -\beta_v kn \frac{dU(1)}{dY}$$

$$\theta(0) = \xi + \beta_v knIn \frac{d\theta(0)}{dY}, \qquad \theta(1) = 1 - \beta_v knIn \frac{d\theta(1)}{dY} \tag{4}$$

where;

$$\beta_v = \frac{2 - f_v}{f_v},\ \beta_t = \frac{2 - f_t}{f_t} . \frac{2\gamma_s}{\gamma_s + 1} . \frac{1}{P_r} \tag{5}$$

$$Kn = \frac{\lambda}{b},\ \ In = \frac{\beta_t}{\beta_v},\ \xi = \frac{T_2 - T_0}{T_1 - T_0} \tag{6}$$

The physical quantities used in the above equations are defined in the nomenclature. However, referring to the values of f_v and f_t given in Eckert and Drake (1972), and Goniak and Duffa (1995), the value of β_v is near unity, and the value of β_t ranges from near 1 to more than 100 for actual wall surface conditions and is near 1.667 for many engineering applications, corresponding to:

$$f_v = 1;\ f_t = 1;\ \ \gamma_s = 1.4 \text{ and } P_r = 0.71. \tag{7}$$

3. Solutions of Governing Equations

3.1 Method of solution (Homotopy Perturbation Method)

To understand and appreciate the basic idea of Homotopy Perturbation Method (HPM), consider the following definitions.

Definition 3.1: Let X , Y be topological spaces and let two continuous maps f, g be defined from X to Y by:

$$f, g: X \to Y$$

A function

$$F : X \times [0, 1] \to Y$$

satisfying $F(x, 0) = f(x)$ and $F(x, 1) = g(x)$ for all $x \in X$

is called a Homotopy from f to g .

Definition 3.2: A set $A \subset R^n$ is said to be convex if for any:

$$x, y \in A; \qquad (1-t)x + ty \in A, \qquad \forall t \in [0, 1]$$

Definition 3.3: Following definitions 3.1 and 3.2, a function

$$F : X \times [0, 1] \to Y$$

defined by $F(x, t) = (1-t) f(x) + tg(x), \qquad \forall x \in X$ and $t \in [0, 1]$

is called convex Homotopy between f and g . Thus, f and g are convex homotopic functions.

With the basic definitions above, we consider now a nonlinear differential equation:

$$A(u) - f(r) = 0,\ r \in \Omega \tag{8}$$

With the boundary condition:

$$B\left(u, \frac{du}{dn}\right) = 0,\ r \in \Gamma \tag{9}$$

where A is a general differential operator, B is a boundary operator, $f(r)$ is a known analytic function, Γ is the boundary of the domain Ω . The operator A can be subdivided into two parts - L and N , where L is the linear and N is the nonlinear operators respectively.

Therefore, (8) can be rewritten as:

$$L(u) + N(u) - f(r) = 0 \tag{10}$$

By the Homotopy technique, a convex Homotopy can be constructed thus:

$$V(r, p) : \Omega \times [0,1] \to R \tag{11}$$

which satisfies: $H(v, p) = (1 - p)[L(v) - L(u_0)] + p[A(v) - f(r)] = 0$ (12)

Or alternatively: $H(v, p) = L(v) - L(u_0) + pL(u_0) + p[N(v) - f(r)] = 0$ (13)

where $r \in \Gamma$ and $p \in [0,1]$ is an embedding parameter, u_0 is an initial guess or approximation of (8) which satisfies the boundary conditions (9).
By (12), it easily follows that:

$$H(v, 0) = L(v) - L(u_0) = 0 \tag{14}$$

and; $$H(v, 1) = A(v) - f(r) = 0 \tag{15}$$

The changing process of p from zero to unity is that of $H(v, p)$ from $L(v) - L(u_0)$ to $A(v) - f(r)$. In other words, $H(v, p)$ continuously traces an implicitly defined curve from a starting point $H(u_0, 0)$ to a solution function $H(f, 1)$. In topology, this changing process is called deformation (Definitions 3.1 to 3.3). Therefore, $L(v) - L(u_0)$ and $A(v) - f(r)$ are called convex Homotopy.
HPM uses $p \in [0, 1]$ as an expanding parameter to obtain

$$V = \sum_{i=0}^{\infty} p^i u_i = u_0 + pu_1 + p^2 u_2 + p^3 u_3 + \ldots \tag{16}$$

And considers the nonlinear term $N(u)$ as

$$N(u) = \sum_{i=0}^{\infty} p^i H_i = H_0 + pH_1 + p^2 H_2 + p^3 H_3 + \ldots \tag{17}$$

where H_n are the He's polynomials which can be calculated by

$$H_n(u_0, \ldots, u_n) = \frac{1}{n!}\frac{\partial^n}{\partial p^n}\left(N\left(\sum_{i=0}^{\infty} p^i u_i \right) \right)_{p=0}, \quad n = 0, 1, 2, \ldots \tag{18}$$

If $p \to 1$, then (16) corresponds to the solution of (8) given by:

$$U = LimV_{p \to 1} = u_0 + u_1 + u_2 + u_3 + \ldots = \sum_{i=0}^{\infty} u_i \tag{19}$$

On the other hand, if $p \to 0$, then (16) reduces to

$$U = \lim_{p \to 0} v = u_0 \tag{20}$$

and becomes the initial guess or approximation of (12)

3.2 Solution process

By HPM, we construct convex Homotopy of equations (1) and (2) respectively as follows.

$$(1-p)[(\frac{d^2U}{dY^2} + \theta) - (\frac{d^2U_0}{dY^2} + \theta_0)] + p(\frac{d^2U}{dY^2} - s\frac{dU}{dY} + \theta) = 0 \tag{21}$$

$$(1-p)(\frac{d^2\theta}{dY^2} + \frac{d^2\theta_0}{dY^2}) + p(\frac{d^2\theta}{dY^2} - s\,\mathrm{Pr}\frac{d\theta}{dY} + Ec.\mathrm{Pr}\left(\frac{dU}{dY}\right)^2) = 0 \tag{22}$$

By (16), the approximate solutions of HPM are given by:

$$U(Y) = U_0 + p^1 U_1 + p^2 U_2 + \ldots \text{ and } \quad \theta(Y) = \theta_0 + p^1\theta_1 + p^2\theta_2 + \ldots \tag{23}$$

By using the appropriate form of (23) in (21) and (22) respectively, expanding and comparing coefficients of equal powers of p yield the following sets of equations with their corresponding boundary conditions.

$$P^0: \quad \frac{d^2U_0}{dY^2} + \theta_0 = 0; \quad U_0(0) = \beta_v Kn\frac{dU_0(0)}{dY}; \quad U_0(1) = -\beta_v Kn\frac{dU_0(1)}{dY} \tag{24}$$
$$\frac{d^2\theta_0}{dY^2} = 0; \quad \theta_0(0) = \xi + \beta_v KnIn\frac{d\theta_0(0)}{dY}; \quad \theta_0(1) = 1 - \beta_v KnIn\frac{d\theta_0(1)}{dY}$$

$$P^1: \quad \frac{d^2U_1}{dY^2} + \theta_1 - s\frac{dU}{dY} = 0; \quad U_1(0) = \beta_v Kn\frac{dU_1(0)}{dY}; U_1(1) = -\beta_v Kn\frac{dU_1(1)}{dY} \tag{25}$$

$$\frac{d^2\theta_1}{dy^2}+\frac{d^2\theta_0}{dy^2}-s\,\mathrm{Pr}\frac{d\theta_0}{dy}+Ec\,\mathrm{Pr}\left(\frac{dU_0}{dy}\right)^2=0;$$

$$\theta_1(0)=\beta_v KnIn\frac{d\theta_1(0)}{dy},\quad \theta_1(1)=-\beta_v KnIn\frac{d\theta_1(1)}{dy}$$

$$P^2:\quad \frac{d^2U_2}{dy^2}+\theta_2-s\frac{dU_1}{dy}=0;\ U_2(0)=\beta_v Kn\frac{dU_2(0)}{dy^2},\quad U_2(1)=-\beta_v Kn\frac{dU_2(1)}{dy^2} \tag{26}$$

$$\frac{d^2\theta_2}{dy^2}-s\,\mathrm{Pr}\frac{d\theta_1}{dy}+2Ec\,\mathrm{Pr}\frac{dU_0}{dy}\frac{dU_1}{dy}=0;$$

$$\theta_2(0)=\beta_v KnIn\frac{d\theta_2(0)}{dy},\qquad \theta_2(1)=-\beta_v KnIn\frac{d\theta_2(1)}{dy}$$

.

$$P^n:\quad \frac{d^2U_n}{dy^2}+\theta_n-s\frac{dU_{n-1}}{dy}=0;\ U_n(0)=\beta_v Kn\frac{dU_n(0)}{dy^2},\ U_n(1)=-\beta_v Kn\frac{dU_n(1)}{dy^2} \tag{27}$$

$$\frac{d^2\theta_n}{dy^2}-s\,\mathrm{Pr}\frac{d\theta_{n-1}}{dy}+Ec\,\mathrm{Pr}\sum_{k=0}^{n-1}\frac{dU_k}{dy}\frac{dU_{n-k-1}}{dy}=0;$$

$$\theta_n(0)=\beta_v KnIn\frac{d\theta_n(0)}{dy},\ \theta_n(1)=-\beta_v KnIn\frac{d\theta_n(1)}{dy},\qquad n\ge 2$$

Solving each pair of equations with their respective boundary conditions beginning with $\theta-equation$ yields:

$$U_0=D+Cy-\frac{B}{2}y^2-\frac{A}{6}y^3 \quad \text{and} \quad \theta_0=B+Ay \tag{28}$$

$$U_1=D_1+C_1y+\frac{f_8y^2}{2!}+\frac{f_9y^3}{3!}+\frac{f_{10}y^4}{4!}-\sum_{i=4}^{7}\frac{f_iy^{i+1}}{(i+1)!} \quad \text{and} \quad \theta_1=B_1+A_1y+\frac{f_1y^2}{2!}+\sum_{i=3}^{6}\frac{f_{i+1}y^i}{i!} \tag{29}$$

$$U_2=D_2+C_2y+\sum_{i=2}^{9}\frac{f_{19+i}y^i}{i!}-\sum_{i=1}^{4}\frac{f_{i+16}y^{i+9}}{(i+9)!} \quad \text{and} \quad \theta_2=B_2+A_2y+\sum_{i=2}^{11}\frac{f_{i+9}y^i}{i!} \tag{30}$$

By using (28), (29) and (30) in (23), the approximate solutions of (1) and (2) are given by:

$$U(y)=g_y+\sum_{i=0}^{8}g_iy^i \quad \text{and} \quad \theta(y)=q_y+\sum_{i=0}^{6}q_iy^i \tag{31}$$

The integration constants used are defined by:

$$A=\frac{1-\varepsilon}{1+2\beta_v KnIn} \qquad B=\frac{\varepsilon\beta_v KnIn+\beta_v KnIn+\varepsilon}{1+2\beta_v KnIn} \qquad C=\frac{1}{2}B+\frac{(1+3\beta_v Kn)A}{6(1+2\beta_v KnIn)}$$

$$D=\beta_v Kn\left[\frac{1}{2}B+\frac{(1+3\beta_v Kn)A}{6(1+2\beta_v KnIn)}\right] \qquad A_1=\frac{-\frac{f_1}{2}-\sum_{i=1}^{4}\left(\frac{f_{i+3}}{(i+2)!}+\beta_v KnIn\left(\frac{f_{i+3}}{(i+1)!}+f_1\right)\right)}{(1+2\beta_v KnIn)}$$

$$B_1=\beta_v KnInA_1 \qquad C_1=\frac{-\sum_{i=1}^{3}\left(\left(\frac{f_{7+i}}{(1+i)!}-\frac{f_{3+i}}{(4+i)!}-\frac{f_7}{8!}\right)+\beta_v Kn\left(\frac{f_{7+i}}{i!}-\frac{f_{3+i}}{(3+i)!}-\frac{f_7}{7!}\right)\right)}{(1+2\beta_v Kn)}$$

$$D_1=\beta_v KnC_1 \qquad A_2=\frac{-\sum_{i=1}^{10}\left(\frac{f_{i+10}}{(i+1)!}+\beta_v KnIn\left(\frac{f_{i+10}}{(i)!}\right)\right)}{(1+2\beta_v KnIn)} \qquad B_2=\beta_v KnInA_2$$

$$C_2=\frac{-\sum_{i=1}^{8}\left(\frac{2+i}{1+i}+\beta_v Kn\right).\frac{f_{20+i}}{i!}+\sum_{i=1}^{4}\left(\frac{10+i}{9+i}+\beta_v Kn\right).\frac{f_{16+i}}{(8+i)!}}{(1+2\beta_v Kn)} \qquad D_2=\beta_v KnC_2 \tag{32}$$

4. Discussion of Results

The approximate solutions of the temperature, velocity, volume flow rate, rate of heat transfer, expressed as local Nusselt number and skin friction are obtained by HPM with the graphs of the results presented in figures 2 – 10. The present problem is governed by Eckert number (Ec) (viscous dissipation parameter), Suction and Injection (s), fluid-wall interaction (*In*), rarefaction or departure from continuum regime ($\beta_v Kn$) and wall ambient temperature difference ratio (ξ). The influences of these parameters especially the Eckert number on the flow regime are discussed with the corresponding figures. The study is carried out over reasonable ranges of $0 \leq \beta vKn \leq 0.2$, $0 \leq \text{In} \leq 13$ and $0 \leq Ec \leq (2\times10)^2$, where $10^{-3} \leq \text{Kn} \leq 10^{-1}$.

Table 4.1: validation of Homotopy perturbation method

Y	AM		HPM ($i=3$)		Absolute Error	
	velocity	Temperature	velocity	Temperature	Velocity	Temperature
0.0	0.0058008814	0.048947115	0.0057934316	0.048936064	0.0744977841	0.0110504245
0.1	0.0202979004	0.123671619	0.0202683608	0.123632167	0.2953961217	0.0394527456
0.2	0.0342709839	0.201096492	0.0342180171	0.201015764	0.5296674266	0.0807273256
0.3	0.0468993716	0.281319317	0.0468284062	0.281198053	0.7096534198	0.1212631947
0.4	0.0572915322	0.364441206	0.0572122459	0.364290230	0.7928632428	0.1509758731
0.5	0.0644804986	0.450566925	0.0644040826	0.450403490	0.7641600045	0.1634348107
0.6	0.0674189252	0.539805025	0.0673554072	0.539649029	0.6351807237	0.1559954310
0.7	0.0649738545	0.632267979	0.0649297711	0.632138044	0.4408342850	0.1299359477
0.8	0.0559211739	0.728072328	0.0558979025	0.727981729	0.2327135584	0.0905991248
0.9	0.0389397473	0.827338820	0.0389328224	0.827291281	0.0692489413	0.0475391600
1.0	0.0126052025	0.930192570	0.0126049603	0.930177897	0.0024211831	0.0146738760
			Error margin:		1.0×10^{-4}	1.0×10^{-3}

Table 1 contains the numerical values of the solutions of velocity and temperature profiles obtained by the analytical method and HPM employed by Jha, et al (2013) and the present study respectively. Suppressing the effect of viscous dissipation in the present problem (i.e., Ec = *0*), the results obtained agree perfectly with those of Jha *et al* (2013). This is evident in the error margin in the order of 1.0×10^{-4} for velocity profile and 1.0×10^{-3} for temperature distribution respectively, as shown in the table.

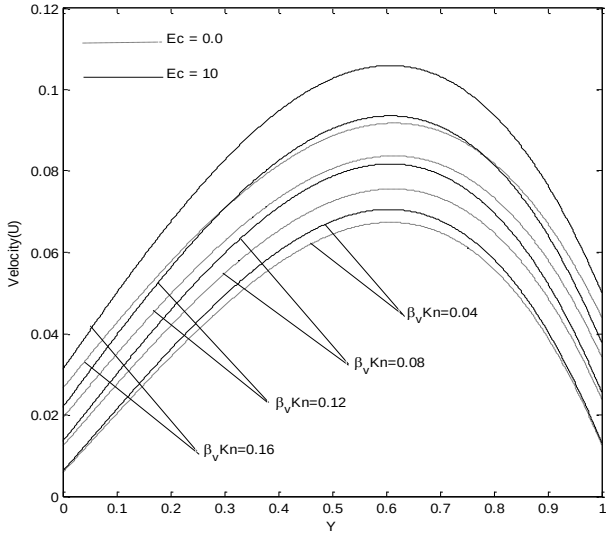

Figure 2: velocity distribution for different values of βvKn at $In = 1.667$, $s = 0.5$, $\Pr = 0.71$, and $\xi = 0.0$.

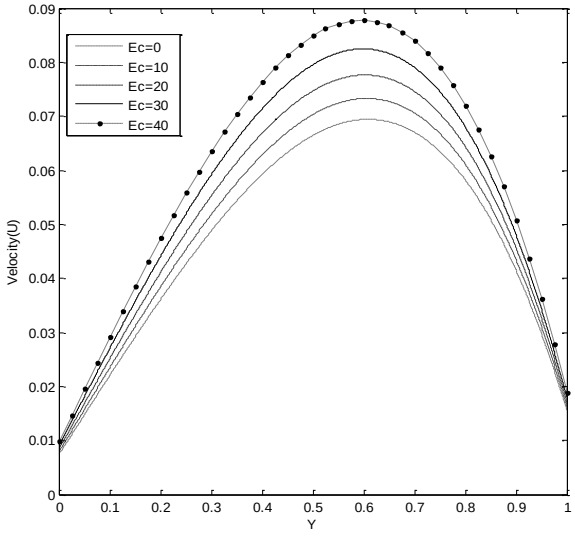

Figure 3: variation of velocity for different values of Ec at $In = 1.667$, $s = 0.5$, $\beta_v Kn = 0.04$, $\Pr = 0.71$, $\xi = 0.0$.

Figures 2 and 3 represent the hydrodynamic behaviour of the fluid across the channel width. Figure 2 shows that fluid velocity increases with increase in Eckert number as well as increasing rarefaction (βvKn). This is attributed to the boundary slip flow at both walls which grows with increasing βvKn. On the other hand, Figure 3 reveals that increasing the viscous dissipation parameter within the flow domain leads to increase in the hydrodynamic behavior of the fluid across the channel width. This is attributed to temperature growth due to internal heat generation caused by the shear heating in the system. This growth in temperature strengthens the convection current, resulting to an increase in the velocity of the system

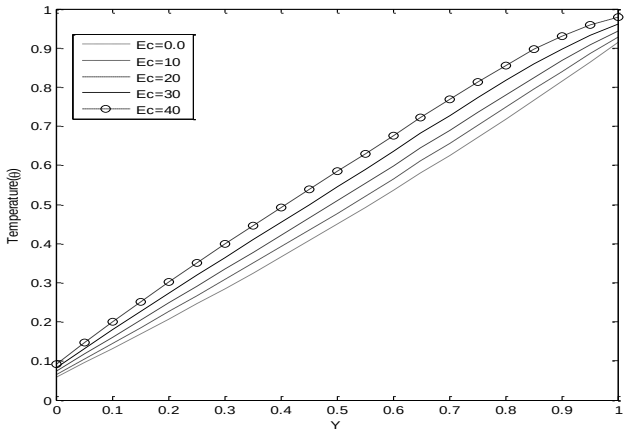

Figure 4: variation of temperature for different values of Ec at fixed values of $s = 0.05$, $\beta vKn = 0.5$, $\Pr = 0.71$, $ln = 1.667$, $\xi = 0.0$.

Figure 4 captures the thermal behavior of the microfluidic flow. A trend similar to that of hydrodynamic behavior of the fluid flow is observed in figure 4 where the thermal characteristics of the fluid is seen to be encouraged and continue to grow with increase in Eckert number. This is physically true for rarefied gas where increase in velocity leads to increase in interactions of fluid particles which enhance the thermal energy of the system.

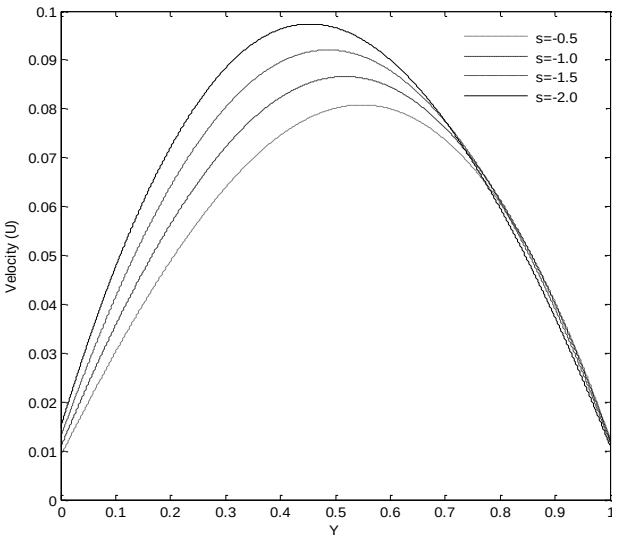

Figure 5: Variation of suction and injection parameter on velocity profile at fixed Ec =1, $\beta_v Kn = 0.04$, $\Pr = 0.71$, $s = 0.5$

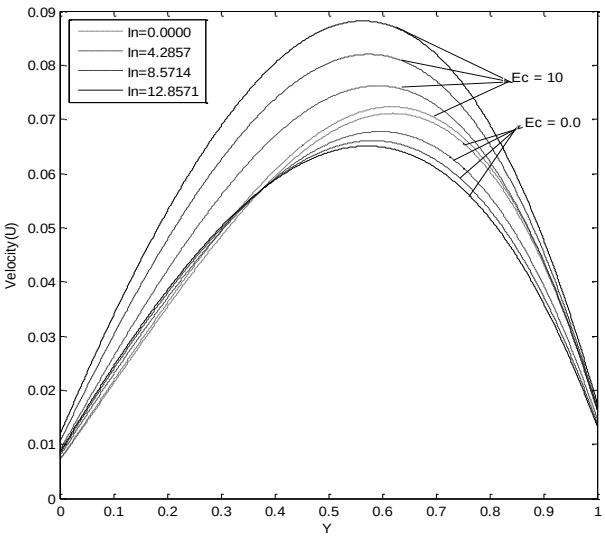

Figure 6: variation of fluid-wall interaction on velocity profile at fixed $\beta vKn = 0.5$, $s = 0.05$, $\Pr = 0.71$, $ln = 1.667$, $\xi = 0.0$

Figure 5 and figure 6 represent the variation of velocity with suction and injection, and fluid wall interaction respectively in the presence of viscous dissipation (Ec > 0). In figure 5, the profile reveals that, increasing

injection through the plate at $Y = 0$ strengthens the velocity of the fluid near the plate at $Y = 0$. However, the influence of injection on the velocity is reduced near the plate at $Y = 1$. This physical situation is true since fresh injected fluid through the porous plate at $Y = 0$ is sucked out through the porous plate at $Y = 1$ just as fluid particles begin to gain energy by the actions of internal shear stress and the temperature (T_1) of the plate.

In figure 6, the growth in the fluid velocity as fluid-wall interaction (*ln*) increases is evident only in the presence of internal shear heating. Where this is absent (Ec = 0 in figure 6), increase in fluid wall interaction is seen to cut down the hydrodynamic strength of the system. It is observed also that the presence of viscous dissipation in this fluid flow reverses the influences of variation of fluid-wall interactions on the velocity of the system. This effect takes place in the region of $Y \geq 0.37$ from the plate defined by $Y = 0$.

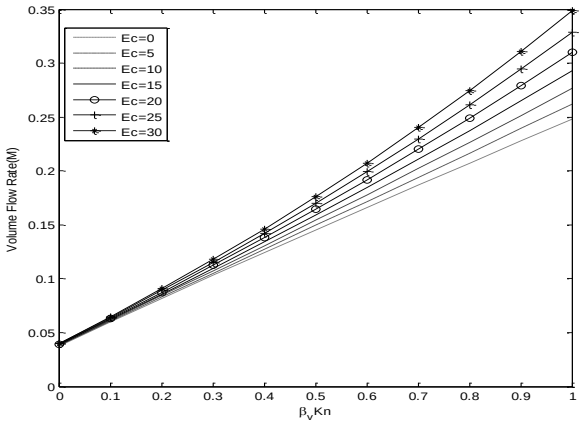

Figure 7: volume flow rate for different values of Ec, $\beta_v Kn = 0.04, \Pr = 0.71,$ $s = 0.5$, $ln = 1.667$, $\xi = 0.0$.

Figure 7 represents the volumetric flow rate for variations of Ec as well as $\beta_v Kn$. The Figure reveals that volumetric flow rate increases with growing $\beta_v Kn$ as well as Ec. It is observed here too that the effect of viscous dissipation parameter (Ec) on volumetric flow rate is negligible at low values of $\beta_v Kn$ but becomes highly significant at large values of $\beta_v Kn$.

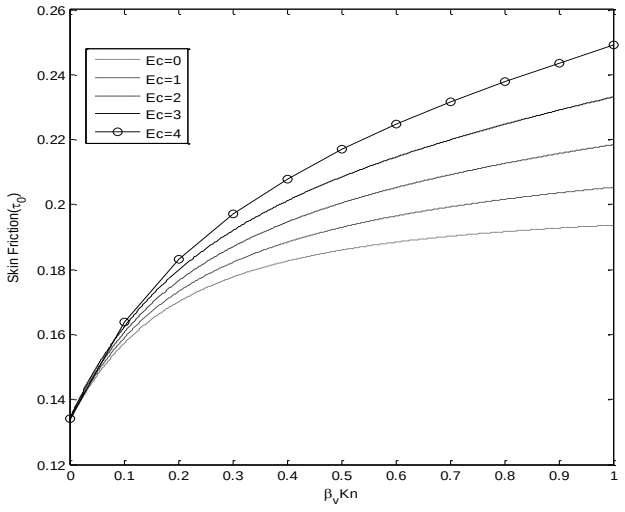

Figure 8a: variation of skin friction at $Y = 0.0$ **for different values of a** Ec **at** $\beta_v Kn = 0.04$, $\Pr = 0.71$, $s = 0.5$, $ln = 1.667$, $\xi = 0.0$.

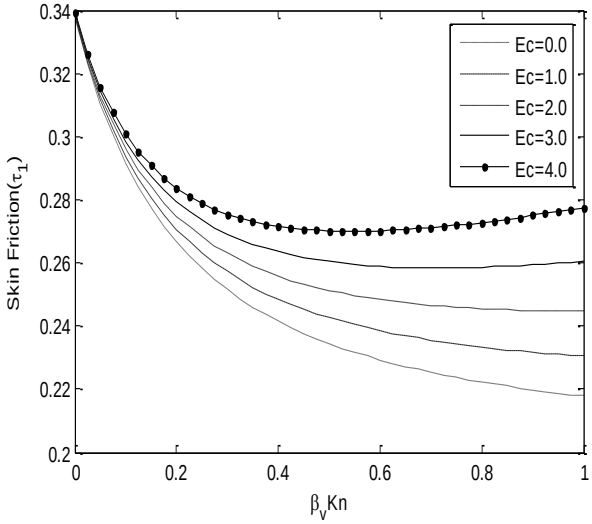

Figure 8b: variation of skin friction $Y = 1.0$ **for different values of** Ec **at** $\beta_v Kn = 0.04$, $\Pr = 0.71$, $s = 0.5$, $ln = 1.667$, $\xi = 0.0$.

In figure 8(a & b), increasing Eckert number causes the skin friction to increase on both channel plates. However, as $\beta_v Kn$ increases, the skin friction at the plate ($Y = 0$) increases while the skin friction at the plate ($Y = 1$) decreases. The trend of the shear stress on the surfaces of the fluid can be attributed to higher velocity gradient obtained near the plate at $Y = 0$ and which decreases as $\beta_v Kn$ increases. As fluid particles flow near the plate at $Y = 1$ in figure 8(b) combined with the actions of internal shear heating, the thermal characteristics of the fluid is strengthened, thus reducing the skin friction of the system at the porous plate defined by $Y = 1$. It is also observed here that the effect of Ec on skin friction is negligible for low values of $\beta_v Kn$ while it is clearly pronounced when the value of $\beta_v Kn$ becomes large.

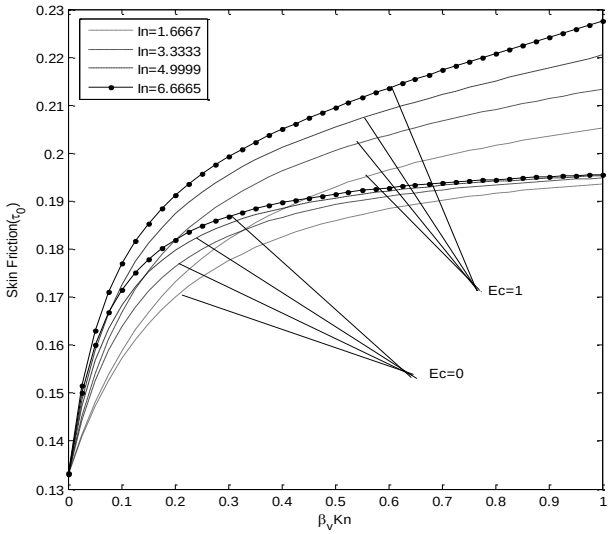

Figure 9a: variation of skin friction for different values of In at $Y = 0.0$, $\beta_v Kn = 0.04$, $\Pr = 0.71$, $s = 0.5$, $\xi = 0.0$

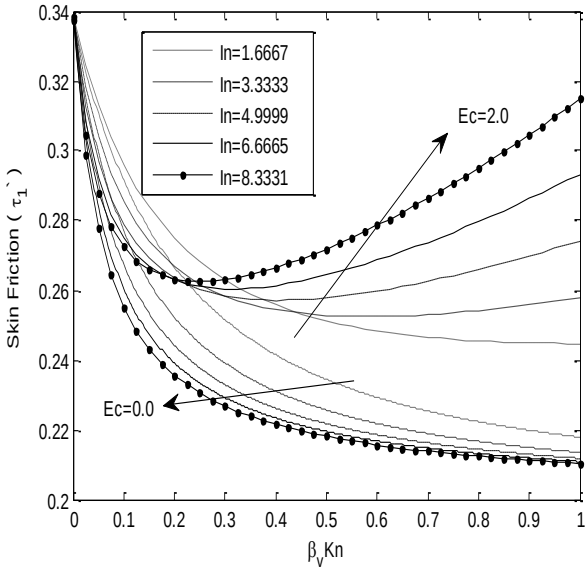

Figure 9b: variation of skin friction for different values of In at $Y = 1.0$, for $\beta_v Kn = 0.04$, $\Pr = 0.71$, $s = 0.5$, $\xi = 0.0$

In Figure 9, the effects of varying fluid-wall interaction (*ln)* in the presence of viscous dissipation is observed to increase the skin friction of the surface of the plate at $Y = 0$ (Figure 9a) as the values of $\beta_v Kn$ become large but weakens the skin friction near the hotter plate (Fig. 9b). This physical situation is attributed to the energy gained by the actions of viscous dissipation in the system. We observed too that viscous dissipation reverses the effect of fluid wall interaction on the skin friction of the system near the plate at $Y = 1$.

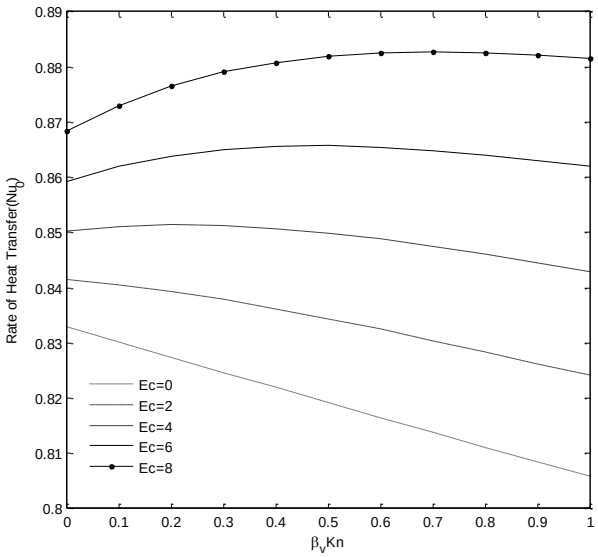

Figure 10a: rate of heat transfer at $Y = 0.0$ for different values of Ec at fixed values of $In = 0.01667,\ \beta_v Kn = 0.04,\ \Pr = 0.71,\ s = 0.5,\ \xi = 0.0$.

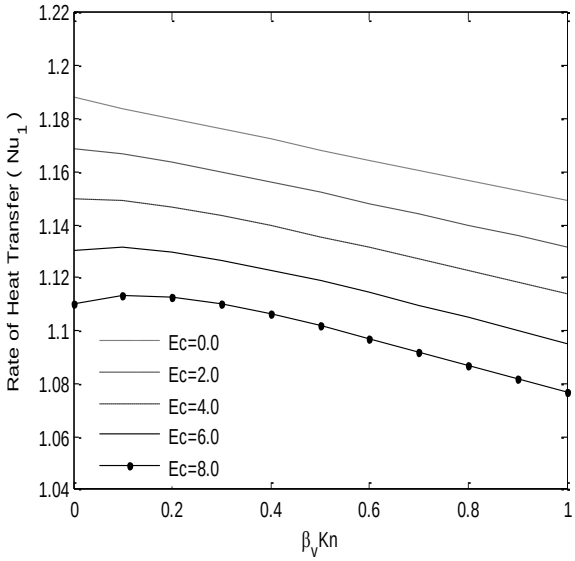

Figure 10b: rate of heat transfer at $Y = 1.0$ for different values of Ec at fixed values of $In = 0.01667,\ \beta_v Kn = 0.04,\ \Pr = 0.71,\ s = 0.5.\ \xi = 0.0$.

Figures 10 represent the variation of rate of heat transfer of the system against the departure from continuum regime ($\beta_v Kn$) at both walls. In the Figures, it is observed that increasing Ec increases the rate of heat transfer of the system at the plate $Y = 0$ in Figure 10(a), while it decreases the rate of heat transfer at the plate $Y = 1$ in Figures 10(b). This is due to the induced buoyancy of the hydrodynamic and thermal strength brought about by the actions of increase in the internal heat generation. This development causes an increase in surface temperature gradient of the fluid near the plate at $Y = 0$ and a reversed phenomenon near the plate at $Y = 1$.

5. Conclusion

This study has examined the effects of viscous dissipation on natural convection flow in a vertical parallel-plate microchannel with suction and injection. Governing equations are developed and appropriate dimensionless parameters are employed to transform the equations into dimensionless forms. The solutions to the dimensionless form steady state energy and velocity equations, which in no wise displayed any closed form solutions, are obtained by HPM. The results of velocity profile, temperature profile, volumetric flow rate, skin friction and rate of heat transfer, expressed as local Nusselt number, are presented in graphs and discussed. The study finds that the presence and variation of viscous dissipation parameter increases the velocity and temperature gradients leading to increase in volume flow rate and rate of heat transfer, even with suction and injection. We observe too that the presence of viscous dissipation in the viscous fluid is more to reverse the influences of the variation of fluid-wall interaction on the velocity and skin friction of the system than reproducing it. This implies that the effect of internal shear heating in any microfluidic flow is significant and should not be neglected. The study also substantiates the findings of the existing literatures that HPM is a powerful tool for solving any system of nonlinear equations arising from the phenomenon of fluid flow. Finally, this study can be conducted in microtubes and in two or three dimensional coordinate geometries.

Reference

1. Chen, C. K. and Weng, H. C., natural convection in a vertical microchannel. *J. Heat Transfer*, 127, 1053 – 1056, 2005Eckert, E. R. G. & Drake, Jr. R. M. (1972), Analysis of Heat and Mass Transfer, New York, McGraw Hill.
2. Haddad, O. M., Abuzaid, M. M. and Al-Nimr, M. A., developing free convection gas flow in a vertical open-ended microchannel filled with porous media. *J. Numerical Heat Transfer, Part A: Applications*, 48(7), 2005
3. Goniak, R. & Duffa, G. (1995), Corrective term in wall-slip equations for Knudsen layer, J. Thermophys. Heat Transfer, 9, 383-384.
4. Jha, B. K. & Ajibade, A. O. (2010), free convective flow between vertical porous plates with periodic heat input. Zamm. z. Angew. Math. Mech., 90(3), 185-193.
5. Jha, B. K., Aina, B. & Joseph, S. B. (2013), natural convection flow in a vertical micro-channel with suction/injection, Proc Imech. E part E: J of Process Mechanical Engineering, 0(0), 1-10.
6. Kakac, S., Kosoy, B., Li, D., and Pramuanjaroenkij, A., Microfluidics Based Microsystems; fundamentals and applications, Springer, http://www.springer.com/978-90-9028-7, 2010.
7. Kargar, A. & Akbarzade, M. (2012), Analytic solution of natural convection flow of a non-Newtonian fluid between two vertical flat plates using HPM, RESEARCH INVENTY: Int'l J. Engineering and sciences, 1(3), 32-38.
8. Motsumi, T. G. & Makinde, O. D. (2012), Effects of thermal radiation and viscous dissipation on boundary layer flow of nanofluids over a permeable moving flat plate, Physical Scripta, 86(4).
9. Murthy, P. V. S. N. & Sigh, P. (1997), effects of viscous dissipation on non-Darcy natural convection regime, Int'l J. of Heat and Mass Transfer, ,40, 1251-1260.
10. Nield, D. A. (2007), the modeling of viscous dissipation in a saturated porous medium, J. of Heat Transfer, 129/1459.
11. Ramiar, V & Ranjbar, A. A. (2011), effects of viscous dissipation and variable properties on nano-fluids flowing two dimensions at micro-channels", IJE Transactions A: Basics, 24, 131-142.
12. Rees, D. A., Magyari, E. and keller, B. (2003), the development of the asymptotic viscous dissipation profile in a vertical free convective boundary layer flow in a porous medium, Transport in Porous Media, 53, 347-355.
13. Shojaefard, M. H., Noorpoor, A. R., Avanesians, A. & Ghaffapour, M. (2005) Numerical investigation of flow control by suction and injection on a subsonic airfoil, Am. J. Applied Sciences, 20(10), 1474-1480.
14. Takhar, H. G. & Beg, O. A. (1997), effects of transverse magnetic field, Prandtl number and Reynolds number on non-Darcy mixed convective flow of an incompressible viscous fluid past a porous vertical flat plate in a saturated porous medium, International Limited J. of Energy Research, 21, 87-100**.**
15. Tunc, V. & Bayazitoglu, Y. (2002), Heat transfer in rectangular microchannels, IJHMT 45(4), 765-773.
16. Uddin, M. J., khan, W. A. and Ismail, A. I. (2013), Effects of dissipation on free convective flow of a non-Newtonian nanofluid in a porous medium with gyolatic micro-organism, Proc Imech E. Part N: J. of Nano Engineering and Nanosystems, 98, 553-564.
17. Vahid, V. Vandadi, A. and Aghanajafi, C. (2011), Slip flow heat transfer in circular microchannel with viscous dissipation, IJRRAS, 6(2).

Ajibade, O. Abiodun (M'99, NMS – M'10, AMS), Born in Zaria on 30th December, 1969. Attended Baptist LSMB Primary School, Ipee, Kwara State (1975-1981), Government Secondary School, Ipee, Kwara State (1981-1986) and Advanced Teachers College, Ahmadu Bello University, Zaria, Kaduna State (1987-1989) for his **First School Leaving Certificate, GCE/OL** and **National Certificate in Education**. He studied at Ahmadu Bello University, Zaria, Kaduna State, Nigeria from 1990 to 2009, where he obtained **B.Sc. (Hons), M.Sc.** and **Ph.D**, all in Mathematics in 1992, 1997, and 2009 respectively. Ajibade O. Abiodun invented a Mathematical concept called: Rhotrix. Major Field of study is Fluid Dynamics.

Otor, D. Omenka, was born in Opiem-Owo, Igede Central District, Oju LGA of Benue State on 1st July, 1980 and attended All Saints Primary School, Umoda Oju, Benue State, Nigeria where he obtained his **First School Leaving Certificate in 1989**. He attended Government Secondary School, Ikachi from 1990-1995 and College of Education, Oju from 1997-2000, all in Oju LGA of Benue State, Nigeria where he obtained **West African Senior Secondary Certificate (WASSC)** and **National Certificate in Education (NCE)** in 1995 and 2000 respectively. Otor, D. Omenka studied at Ahmadu Bello University, Zaria, Kaduna State, Nigeria from 2004-2008 for his **B.Sc.(Ed) Mathematics** and from 2011-2017 for his **M.Sc. Mathematics**. Major Field of study is Fluid Dynamics.

NOMENCLATURE/GREEK LETTERS

b	channel width
Y	dimensionless y - coordinate
C_p , C_v	specific heats at constant pressure and constant volume, respectively
f_t , f_v	thermal and tangential momentum accommodation coefficients respectively
g	gravitational acceleration
In	fluid – wall interaction, (β_t / β_v)
Kn	Knudsen number
m	volume flow rate
M	dimensionless volume flow rate
Nu	rate of heat transfer (Nusselt Number)
Pr	Prandtl number
Ec	Eckert number (viscous dissipation parameter)
s	suction/injection parameter
T	temperature of fluid
v, u	velocity components in x, y directions
V_0	constant suction/injection velocity
U	dimensionless velocity
U_0	dimensionless reference velocity

Greek symbols

λ	particle mean free path
α	thermal diffusivity
β	thermal expansion coefficient
β_t , β_v	dimensionless variables
γ_s	ratio of specific heat (C_p/C_v)
Θ	dimensionless temperature
μ	dynamic viscosity
ν	fluid kinematic viscosity
ξ	wall – ambient temperature difference ratio
ρ	density

Subscripts

T_0	reference temperature
T_1	temperature of the hotter wall
T_2	temperature of the colder wall